

THE SCHLÄFLI FAN

MICHAEL JOSWIG, MARTA PANIZZUT, AND BERND STURMFELS

ABSTRACT. Smooth tropical cubic surfaces are parametrized by maximal cones in the unimodular secondary fan of the triple tetrahedron. There are 344 843 867 such cones, organized into a database of 14 373 645 symmetry classes. The Schläfli fan gives a further refinement of these cones. It reveals all possible patterns of lines on tropical cubic surfaces, thus serving as a combinatorial base space for the universal Fano variety. This article develops the relevant theory and offers a blueprint for the analysis of big data in tropical geometry.

1. INTRODUCTION

A cubic surface in projective 3-space \mathbb{P}^3 is the zero set of a cubic polynomial

$$(1) \quad \begin{aligned} & c_0 w^3 + c_1 w^2 z + c_2 w z^2 + c_3 z^3 + c_4 w^2 y + c_5 w y z + c_6 y z^2 + c_7 w y^2 + c_8 y^2 z + c_9 y^3 + c_{10} w^2 x \\ & + c_{11} w x z + c_{12} x z^2 + c_{13} w x y + c_{14} x y z + c_{15} x y^2 + c_{16} w x^2 + c_{17} x^2 z + c_{18} x^2 y + c_{19} x^3. \end{aligned}$$

Here $(w : x : y : z)$ are homogeneous coordinates on \mathbb{P}^3 . George Salmon and Arthur Cayley discovered in the 1840s that every smooth cubic surface contains 27 lines. Ludwig Schläfli studied the combinatorics of the lines in his 1858 article [23]. The name of that Swiss mathematician appears in our title.

This article is dedicated to the memory of Branko Grünbaum. Grünbaum is famous for his work on polytopes and arrangements, especially those that admit a high degree of symmetry. In the literature on these geometric figures, one sees a direct line connecting Ludwig Schläfli to Branko Grünbaum. This is highlighted by the use of the *Schläfli symbol* for symmetries of polyhedra.

The combinatorial strand of algebraic geometry underwent a major shift during the past two decades, thanks to the advent of tropical geometry [18]. The following question emerged early on during the tropical revolution: *What are all shapes of smooth cubic surfaces in tropical 3-space, and which arrangements of tropical lines occur on such surfaces?* A first guess is that there are 27 lines, just like in the classical case. But this is false. Vigeland [24] showed that the number of lines can be infinite. A textbook reference is [18, Theorem 4.5.8].

The aim of this article is to give a comprehensive answer to the questions above. We will do so via a computational study of all smooth tropical cubic surfaces. These surfaces are dual to unimodular regular triangulations of the *triple tetrahedron* $3\Delta_3$, which is the Newton polytope of the cubic polynomial seen in (1). The relevant definitions will be reviewed in Section 2.

Our point of departure is the article [22], which classifies the ten motifs that describe the potential positions of a tropical line on a cubic surface. These motifs are denoted 3A, 3B, ..., 3J. They are shown in Table 1. The advance we report in this paper is a large-scale computation that identifies the motifs of all lines that actually occur on the many tropical smooth cubic surfaces.

Our contribution rests on earlier work by Jordan et al. [16] who developed highly efficient tools for enumerating triangulations. Their count for $3\Delta_3$ in [16, Theorem 19] shows that there are 14 373 645 combinatorial types of smooth tropical cubic surfaces. Here, the types are the orbits of the symmetric group S_4 by permuting w, x, y, z in the 20 terms of (1). Adding up the sizes of all S_4 -orbits, we obtain the total number 344 843 867 of smooth tropical cubics.

This article is organized as follows. In Section 2 we fix notation, we discuss unimodular triangulations of the tetrahedron $3\Delta_3$, and we review basics on lines and surfaces in tropical projective space \mathbb{TP}^3 . We also recall the classification of motifs in [22]. Section 3 furnishes our classification of smooth tropical cubic surfaces. This is presented in Theorem 3.1, and it is followed by a detailed explanation of the methodology that underlies our work and its results.

Section 4 studies occurrences of motifs in the unimodular triangulations of $3\Delta_3$. Our main result is Theorem 4.1. We present an algorithm for computing occurrences. This rests on several lemmas that describe geometric constraints. The algorithm is applied to all triangulations in Theorem 3.1. As a consequence, we get a complete list of occurrences of motifs for each of the 14 373 645 types.

In Section 5 we zoom in on particular secondary cones. For each cubic surface of one type, an occurrence of a motif may be visible or not. Being visible means that there exists a line for that motif. Hence, for any specific surface, only a subset of the motifs occurring in the triangulation is visible. The regions on which that subset is constant are convex polyhedral cones. These form the Schläfli fan. Thus, each of the 14 373 645 secondary cones is divided into its Schläfli cones. We present and discuss the result of that computation.

Our combinatorial and computational study in this paper lays the foundation for future work on the nonarchimedean geometry of classical cubic surfaces over a valued field. In Section 6 we take a step into that direction. We discuss the universal Fano variety and the universal Brill variety, and we examine the tropical discriminants of these universal families. The first version of this article had a Section 7 which proposed a normal form for cubic surfaces, called the eight-point model. This was deleted in this final version because an even better such model was found in the subsequent project [21] with Emre Sertöz.

The methods from computer algebra and polyhedral geometry which led to our results are at the forefront of what is currently possible in terms of hardware, algorithms and software. For instance, to determine and analyze the regular unimodular triangulations of $3\Delta_3$ took more than 200 CPU days on an Intel Xeon E5-2630 v2 cluster. Yet the most difficult question we had to answer was how to make the results of such a large computation available to others. For this we set up a `polymake` extension `TropicalCubics` [17] and a database within the `polyDB` framework [20]. They can be accessed via `polymake` [8]. The database can also be used via an independent API. We believe that this approach can serve as a model for sharing “big data” in mathematical research.

2. TRIANGULATIONS, CUBIC SURFACES AND TROPICAL LINES

In this section we review the basics and known results on which our study rests. For conventions on tropical geometry we follow the textbook by Maclagan and Sturmfels [18]. Our tropical semiring is the min-plus algebra $(\mathbb{R} \cup \{\infty\}, \oplus, \odot)$. We use upper case letters to denote tropical variables and coefficients. Our orderings of variables and monomials are consistent with the conventions used by `polymake` [8]. For instance, here is a homogeneous

tropical cubic polynomial:

$$(2) \quad \begin{aligned} &44W^3 \oplus W^2Z \oplus 1WZ^2 \oplus 15Z^3 \oplus 19W^2Y \oplus WYZ \oplus 9YZ^2 \\ &\oplus 2WY^2 \oplus 4Y^2Z \oplus Y^3 \oplus 38W^2X \oplus WXZ \oplus 15XZ^2 \oplus 16WXY \\ &\oplus 4XYZ \oplus 1XY^2 \oplus 33WX^2 \oplus 16X^2Z \oplus 14X^2Y \oplus 29X^3. \end{aligned}$$

The expression (2) is evaluated in classical arithmetic as follows:

$$\min\{44+3W, 2W+Z, 1+W+2Z, 15+3Z, \dots, 14+2X+Y, 29+3X\}.$$

The surface defined by (2) is the set of all points (W, X, Y, Z) for which this minimum is attained at least twice. That tropical cubic surface lives in the tropical projective torus $\mathbb{R}^4/\mathbb{R}\mathbf{1}$, but it also has a natural compactification in the tropical projective space \mathbb{TP}^3 . The latter is described in [18, Chapter 6].

A standard reference for the material that follows next is the textbook by De Loera, Rambau and Santos [4]. Reading the coefficients of the tropical polynomial as a height function defines a regular polyhedral subdivision of the 20 lattice points in $3\Delta_3$. If the coefficients are generic enough then the dual subdivision is a triangulation. For now the latter property may be taken as a definition for *generic*; it is a main point of later sections to refine this. If each of its tetrahedra has unit normalized volume, then the triangulation is *unimodular* and the tropical cubic surface is *smooth*. Every unimodular triangulation T of the configuration $3\Delta_3$ has the same f-vector $f(T) = (20, 64, 72, 27)$. Its boundary has the f-vector $f(\partial T) = (20, 54, 36)$. From this we conclude that every smooth tropical cubic surface has 27 vertices, 36 edges, 36 rays, 10 bounded 2-cells, and 54 unbounded 2-cells. This is the case $d = 3$ in [18, Theorem 4.5.2]. Specifically, the $64 - 54 = 10$ interior edges of T correspond to the bounded polygons in the surface. These 10 polygons form the bounded complex of the tropical surface. This is also known as the *tight span*. For cubics, it is contractible. We define the *B-vector* of the triangulation T to be (b_3, b_4, b_5, \dots) , where b_j denotes the number of j -gons in the tight span. The *GKZ-vector* is $(g_0, g_1, \dots, g_{19})$, where g_i is the number of tetrahedra containing point i .

Example 2.1. The tropical cubic polynomial in (2) is identified with its coefficient vector $(44, 0, 1, 15, 19, 0, 9, 2, 4, 0, 38, 0, 15, 16, 4, 1, 33, 16, 14, 29)$. This defines a unimodular triangulation T of $3\Delta_3$. Its 27 tetrahedra are given by their labels:

$$(3) \quad \begin{aligned} &\{0, 1, 4, 10\}, \{1, 2, 5, 11\}, \{1, 4, 7, 13\}, \{1, 4, 10, 16\}, \{1, 4, 13, 19\}, \{1, 4, 16, 19\}, \{1, 5, 9, 11\}, \\ &\{1, 7, 9, 15\}, \{1, 7, 13, 18\}, \{1, 7, 15, 18\}, \{1, 9, 11, 15\}, \{1, 11, 15, 18\}, \{1, 11, 18, 19\}, \{1, 13, 18, 19\}, \\ &\{2, 3, 6, 14\}, \{2, 3, 11, 14\}, \{2, 5, 9, 11\}, \{2, 6, 8, 14\}, \{2, 8, 9, 14\}, \{2, 9, 11, 15\}, \{2, 9, 14, 15\}, \\ &\{2, 11, 14, 15\}, \{3, 11, 12, 14\}, \{11, 12, 14, 17\}, \{11, 14, 15, 17\}, \{11, 15, 17, 18\}, \{11, 17, 18, 19\}. \end{aligned}$$

The GKZ-vector equals $(1, 14, 9, 3, 5, 3, 2, 4, 2, 7, 2, 14, 2, 4, 9, 9, 2, 4, 7, 5)$. The last entry 5 means that the label 19 occurs five times in (3). The B-vector of (3) is $(2, 4, 2, 2)$. To see this, we list the ten interior edges and their links:

$$\begin{array}{llll} \{1, 13\}, [4, 7, 18, 19] & \{1, 15\}, [7, 9, 18, 11] & \{1, 18\}, [7, 13, 19, 11, 15] & \{2, 14\}, [3, 6, 8, 9, 15, 11] & \{2, 15\}, [9, 11, 14] \\ \{9, 11\}, [1, 5, 2, 15] & \{11, 18\}, [1, 15, 17, 19] & \{11, 14\}, [2, 3, 12, 17, 15] & \{11, 15\}, [1, 9, 2, 14, 17, 18] & \{5, 11\}, [1, 2, 9] \end{array}$$

The *link* of an edge e in T is the graph of all edges in T whose union with e is a tetrahedron in T . If e is an interior edge of T , then this graph is a cycle. For instance, the link of $\{9, 11\}$ is the 4-cycle $\{\{1, 5\}, \{5, 2\}, \{2, 15\}, \{15, 1\}\}$. The corresponding bounded 2-cell in the tropical cubic surface is a quadrilateral. The triangulation (3) lies in the same S_4 -orbit as the one featured in [14, §6.2].

Each of the 36 bounded edges of the surface determines a linear inequality among the coefficients C_0, C_1, \dots, C_{19} , expressing that the edge has positive length. The *secondary cone* $\text{sec}(T)$ is the set of solutions to these inequalities. This is a full-dimensional cone in \mathbb{R}^{20} with 4-dimensional lineality space. The number of facets of $\text{sec}(T)$ is between 16 and 36. The secondary cone of the triangulation (3) has 16 facets. It contains the coefficient vector of (2).

The symmetric group S_4 acts naturally on the 20 points in $3\Delta_3$. This induces an action on the set of all triangulations. Note that S_4 also acts on the set of GKZ-vectors. The S_4 -orbit of the triangulation T from (3) has size 24. Equivalently, the stabilizer of T is trivial. The census of unimodular triangulations and associated cubic surfaces is presented in Theorem 3.1.

We now come to tropical lines in 3-space. Vigeland started the classification of how such lines can lie on generic smooth tropical cubic surfaces. Based on a massive random search with `polymake`, Simon Hampe realized that the classification was not complete. The triangulation (3) occurred in the joint article [14] as the first explicit counter-example to Vigeland's list. The final characterization is due to Panizzut and Vigeland [22]. Their list of ten motifs is reproduced in Table 1. This table forms the foundation for our present study.

We identify \mathbb{R}^3 with $\mathbb{R}^4/\mathbb{R}\mathbf{1}$ by setting $\omega_0 = -(e_1 + e_2 + e_3)$, $\omega_1 = e_1$, $\omega_2 = e_2$ and $\omega_3 = e_3$. A *tropical line* in \mathbb{R}^3 is a balanced polyhedral complex given by two 3-valent adjacent vertices, joined by one bounded edge, and four rays with directions $\omega_0, \omega_1, \omega_2$ and ω_3 . If the bounded edge has length zero, the tropical line is *degenerate*. Non-degenerate lines come in three labeled types, given by the direction of the bounded edge. This direction is either $\omega_0 + \omega_1 = -\omega_2 - \omega_3$ or $\omega_0 + \omega_2 = -\omega_1 - \omega_3$ or $\omega_0 + \omega_3 = -\omega_1 - \omega_2$. We denote these three types by $01|23$, $02|13$ and $03|12$. This is shown in Figure 1.

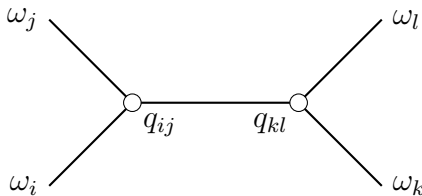


FIGURE 1. A non-degenerate tropical line of labeled type $ij|kl$ in 3-space.

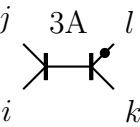
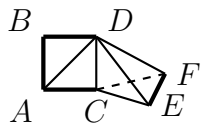
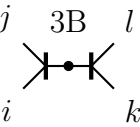
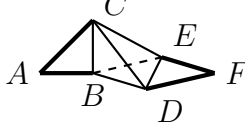
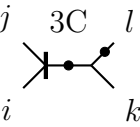
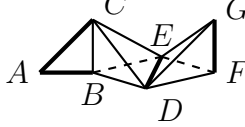
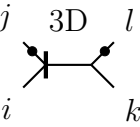
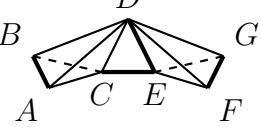
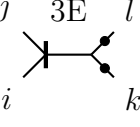
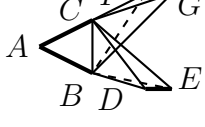
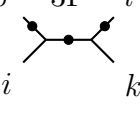
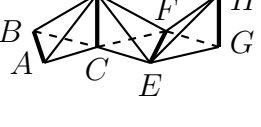
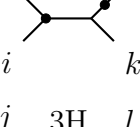
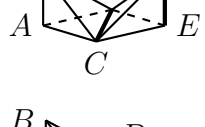
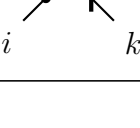
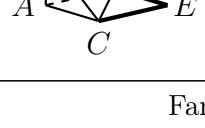
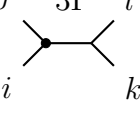
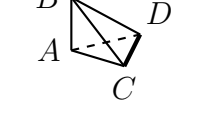
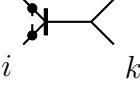
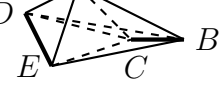
Each tropical line L in \mathbb{R}^3 is encoded (up to tropical scaling) by its *tropical Plücker vector* $P = (P_{01}, P_{02}, P_{03}, P_{12}, P_{13}, P_{23}) \in \mathbb{R}^6$. The six P_{ij} are the tropical 2×2 minors of a 2×4 -matrix. A vector $P \in \mathbb{R}^6$ is the tropical Plücker vector of a line if and only if it lies on the tropical hypersurface given by

$$(4) \quad P_{01} \odot P_{23} \oplus P_{02} \odot P_{13} \oplus P_{03} \odot P_{12}.$$

This means that the minimum in (4) is attained at least twice. Equivalently, P is a height function on the six vertices of the regular octahedron which induces a split into two Egyptian pyramids [18, Figure 4.4.1]. The tropical hypersurface defined by (4) is the tropical Grassmannian $\text{Trop}(G^0(2, 4))$.

A tropical line L is recovered from its Plücker vector $P \in \mathbb{R}^6$ as follows. We start by identifying the pair of terms in (4) which attains the minimum. Suppose $P_{01} + P_{23} = P_{02} + P_{13} \leq P_{03} + P_{12}$, i.e., the labeled type is $03|12$. Then, by [18, Example 4.3.19], L consists of the

TABLE 1. The ten motifs from [22] for tropical lines on generic cubic surfaces.

Marked Lines	Associated Motifs	Necessary Conditions
Isolated Lines		
j  i		Exits: $AB \subseteq F_i$, $BD \subseteq F_j$, $AC \subseteq F_k$, $EF \subseteq F_l$, $AD \subseteq \{x_i + x_j = 1\}$, $CD \subseteq \{x_l = 1\}$, $A \neq E, F$ and $B \neq C$.
j  i		Exits: $AB \subseteq F_i$, $AC \subseteq F_j$, $DF \subseteq F_k$, $EF \subseteq F_l$, $BC \subseteq \{x_i + x_j = 1\}$, $DE \subseteq \{x_k + x_l = 1\}$, $A \neq D, E$ $F \neq B, C$ and $A \neq F$.
j  i		Exits: $AB \subseteq F_i$, $AC \subseteq F_j$, $DE \subseteq F_k$, $FG \subseteq F_l$, $BC \subseteq \{x_i + x_j = 1\}$, $DE \subseteq \{x_l = 1\} \cap F_k$, $A \neq D, E$.
j  i		Exits: $CE \subseteq F_i$, $AB \subseteq F_j$, $DE \subseteq F_k$, $FG \subseteq F_l$, $CD \subseteq \{x_j = 1\}$, $DE \subseteq \{x_l = 1\} \cap F_k$, $E \neq A, B$.
j  i		Exits: $AB \subseteq F_i$, $AC \subseteq F_j$, $DE \subseteq F_k$, $FG \subseteq F_l$, $BC \subseteq \{x_k = 1\} \cap \{x_l = 1\}$.
j  i		Exits: $CD \subseteq F_i$, $AB \subseteq F_j$, $EF \subseteq F_k$, $GH \subseteq F_l$, $CD \subseteq \{x_j = 1\} \cap F_i$, $EF \subseteq \{x_l = 1\} \cap F_k$.
j  i		Exits: $CD \subseteq F_k$, $EF \subseteq F_l$, $ABCD$ has exits also in F_i and F_j , $CD \subseteq \{x_l = 1\} \cap F_k$.
j  i		Exits: $CE \subseteq F_k$, $DE \subseteq F_l$, $ABCD$ has exits also in F_i and F_j , $CD \subseteq \{x_k + x_l = 1\}$, $E \neq A, B$.
Families of Lines		
j  i		Exits: $CD \subseteq F_k \cap F_l$, $ABCD$ has exits also in F_i and F_j .
j  i		Exits: $BC \subseteq F_i \cap F_j$, $DE \subseteq F_k \cap F_l$, $AD \subseteq \{x_j = 1\}$, $AE \subseteq \{x_i = 1\}$.

segment joining the two points

$$(5) \quad \begin{aligned} q_{03} &= (P_{02} + P_{03}, P_{02} + P_{13}, P_{02} + P_{23}, P_{03} + P_{23}) \quad \text{and} \\ q_{12} &= (P_{02} + P_{13}, P_{12} + P_{13}, P_{12} + P_{23}, P_{13} + P_{23}) \quad \text{in } \mathbb{R}^4/\mathbb{R}\mathbf{1} \end{aligned}$$

and the four rays $q_{03} + \mathbb{R}_{\geq 0} \cdot \omega_0$, $q_{03} + \mathbb{R}_{\geq 0} \cdot \omega_3$, $q_{12} + \mathbb{R}_{\geq 0} \cdot \omega_1$, $q_{12} + \mathbb{R}_{\geq 0} \cdot \omega_2$. The formulas for the other two labeled types, 01|23 and 02|13, are analogous.

In summary, the vertices q_{ij} and q_{kl} of a tropical line L are computed from the Plücker coordinates in (5). Conversely, the Plücker vector is obtained by taking the tropical 2×2 minors of the 2×4 -matrix with rows q_{ij} and q_{kl} .

The article [22] describes the various ways in which a tropical line L can lie on a smooth cubic surface S in 3-space. Here we require S to be generic in the precise sense of Section 5. On the line L we mark the points where L intersects edges or vertices of the surface S . These are the bars and dots indicated on the tropical lines in the left column of Table 1. Each bar is dual to a triangle in T , and each dot is dual to a tetrahedron in T . Formally, a *motif* of a tropical cubic surface is one of the ten abstract simplicial complexes 3A, 3B, ..., 3J which are listed in the middle column of Table 1. Each is equipped with a labeling of its vertices by A, B, \dots and a marking of precisely four edges by i, j, k, l . That this list of ten motifs is complete is the main result of [22].

The number of vertices of the ten motifs range between four and eight; the marked edges are the *exits* of the motif. The names of the motifs all start with the digit 3 to indicate the degree of the tropical surface; there are more motifs for other degrees [22, Table 2]. The article [22] distinguishes between “primal motifs” and “dual motifs”. We use the term motif for what is called “dual motif” in [22]. Our Table 1 uses x_i, x_j, x_k, x_l for the homogeneous coordinates of the lattice points in $3\Delta_3$, and it uses the notation $F_i = \{x \in 3\Delta_3 \mid x_i = 0\}$ for the facets of $3\Delta_3$. The third column of Table 1 explicates additional conditions to be satisfied by some edges in order for the motif to occur in T . These are derived in [22, Proposition 23]. They will become important in Section 4.

3. DATA, SOFTWARE, AND LINES ON CUBICS

A primary goal of the present work is to present a database for smooth tropical cubic surfaces. We now explain our database and the underlying methodology. We start with the classification of combinatorial types. The proof of this result is the computation reported in [16, Theorem 19], plus an analysis of the orbits.

Theorem 3.1. *The triple tetrahedron $3\Delta_3$ has precisely 344 843 867 regular unimodular triangulations. These are grouped into 14 373 645 orbits with respect to the natural action of S_4 . The distribution of orbit sizes is shown in Table 2.*

TABLE 2. Distribution of orbit sizes among smooth tropical cubic surfaces: 99.93% of the combinatorial types have no symmetry, i.e., the orbit size is 24.

3	4	6	8	12	24
3	15	25	82	10124	14363396

Remark 3.2. Each smooth tropical cubic surface in $\mathbb{R}^4/\mathbb{R}\mathbf{1}$ has four elliptic curves in its boundary in \mathbb{TP}^3 . These are the tropical plane cubics which are dual to the induced triangulations of the ten lattice points in the triple triangle $3\Delta_2$. That configuration has precisely 79 unimodular triangulations, all of which are regular. They are grouped into 18 orbits with respect to the natural action of S_3 . Hence, we encounter at most $79^4 = 38\,950\,081$ triangulations of the boundary $\partial(3\Delta_3)$. This means that, on the average, more than eight regular unimodular triangulations of $3\Delta_3$ induce the same boundary triangulation.

Before we enter the technical details, we briefly pause to reflect on the nature of a result like Theorem 3.1, how it can be useful, and to what extent it can be trusted. Theorem 3.1 is a highly condensed statement which was derived from massive computations, partially on large clusters, and the total time spent exceeds several months. Most readers will not have access to these types of hardware and technical resources and therefore will be unable to repeat these computations on their own. As we see it, the bulk of the data is the actual theorem. Theorem 3.1 is a mere corollary which follows from something which is too large to write down in any article. That data and more is made publically available at

(6) <https://db.polymake.org/>

to allow everyone to derive their own corollaries. We stress that *all* the software that was used in the process is open source. Therefore, the entire proof of Theorem 3.1, which consists of software and data (in addition to this text), is available for scrutiny. Ideally, such a computer proof would be formalized, but currently this seems to be out of scope for a project of this size. Turning this into a formal proof would be a large project on its own, probably much larger than `flyspeck` [7], if feasible at all. This leaves the question of correctness.

As we see it, making data available and documenting this in an article is a necessary first step. Everyone is invited to probe the data for its correctness; we prepared various tools, explained below, to help with the probing. Any errors found in the future will be corrected in the data base. It would be desirable to have a general mechanism for this, accepted by the mathematical community. Finally, we would like to point out that it was a massive `polymake` experiment run by Simon Hampe which lead to the triangulation (3), which exhibited a flaw in a first version of [22]. That may be seen as a predecessor to this project.

High-level view on the data computed. For each of the 14 373 645 triangulations T in our database, the following annotations are reported: the GKZ-vector, the B-vector, the orbit size with respect to the S_4 -action, and a unique *identifier*. The identifier is an integer between 1 and 14 373 645, which can be used to retrieve the triangulation and data derived. Frequently we will use the symbol ‘#’ for marking identifiers. The triangulation (3) has the identifier #5054117.

The facets of each triangulation are listed in lexicographic order. The representative for a combinatorial type is chosen such that the GKZ-vector is lexicographically minimal. Another important item in our database is a vector $C \in \mathbb{N}^{20}$ of minimum coordinate sum in the interior of each secondary cone. In order to find this vector, we had to solve an integer linear programming problem. We did this using the software `SCIP` [11]. The coefficients of the tropical polynomial (2) were derived from the triangulation (3) in this way. Note that, by construction, C is always generic in the sense that the regular subdivision induced is a triangulation. However, it is *not* generic as defined in Section 5.

Exploring the database. We now describe how to access the data we produced. We offer a collection **SchlaefliFan** within the database **Tropical** of **polyDB** [20]. The simplest possible access is by directing a standard web browser to (6). However, for best results, we recommend the concurrent use of a recent version of **polymake** [8]. The new **polymake** extension **TropicalCubics** [17] is the software companion to this paper. It is available from and further explained at <https://polymake.org/doku.php/extensions/tropicalcubics>. Future additions will deal with other aspects of tropical cubic surfaces.

TABLE 3. Data for some triangulations. The first row is the triangulation (3), and the second one is the honeycomb triangulation from Example 3.3 below. The next two are combinatorially non-isomorphic but share the same canonical hash values. The final two are combinatorially isomorphic but in distinct orbits.

Identifier	Canonical Hash	Altshuler Determinant
#5054117	81 541 384	614 912
#12369387	1 464 729 205	0
#1957163	1 000 016 429	278 528
#3315847	1 000 016 429	684 032
#10720721	1 000 063 702	560 512
#14051499	1 000 063 702	560 512

One pertinent question is how to find a given triangulation T in the database. The user is unlikely to know the search key, and T may be given by its list of facets as in (3). One way is to compute the GKZ-vector and to then generate the lexicographically minimal representative within its S_4 -orbit. This is the preferred method since it identifies the regular triangulation uniquely. Thus, in practice, the lex-minimal GKZ-vector works as another search key. An alternative method is to find a canonical form of T as a simplicial complex. This means identifying the isomorphism type of the incidence graph of the 20 vertices and the 27 tetrahedra. The software **nauty** [19] is a standard tool for this task. It computes a *canonical hash* value, which is a 64-Bit integer that encodes the isomorphism type. This hash value is also stored in our database. It can be used as an index to retrieve a triangulation instantly; cf. Table 3.

The canonical hash value is a combinatorial invariant, but it is not unique. Table 3 shows two triangulations with the same hash value. Nonetheless, they are not isomorphic as abstract simplicial complexes, as can be seen as follows. Let v_1, v_2, \dots, v_k and t_1, t_2, \dots, t_l be an ordering of the vertices and the facets, respectively, of a simplicial complex T . The *incidence matrix* J is the 0/1-matrix with $J_{ij} = 1$ if vertex v_i lies on the facet t_j and $J_{ij} = 0$ otherwise. We define the *Altshuler determinant* of T to be $\max(|\det(JJ^\top)|, |\det(J^\top J)|)$. This number does not depend on the orderings [1, Theorem 3]. It is a combinatorial invariant of T . This distinguishes the third and fourth triangulations in Table 3. Our database can be queried for Altshuler determinants directly.

It also happens that two abstractly isomorphic triangulations lie in different S_4 -orbits. A pair of examples is given at the end of Table 3. Altogether there are 79 572 hash values (i.e.,

about 0.5%) that correspond to two or more S_4 -orbits of triangulations. The maximal multiplicity of any hash value is four. So, with high probability, **nauty** identifies the triangulation uniquely.

Lines in surfaces. We now shift gears, with a discussion of the following basic problem. Given a non-degenerate tropical line L and a tropical cubic surface S , decide whether S contains L . We present an algorithm that solves this.

Let $\ell(t) = [\ell_0(t), \ell_1(t), \dots, \ell_m(t)]$ be an ordered list of linear polynomials $\ell_i(t) = \alpha_i t + \beta_i$. An interval U in \mathbb{R} is *covered by* $\ell(t)$ if the minimum value in the list $\ell(u)$ is attained at least twice for all $u \in U$. This can only happen if some $\ell_i(t)$ appear multiple times in $\ell(t)$. We introduce the *coincidence partition*

$$(7) \quad \{0, 1, \dots, m\} = \sigma_1 \dot{\cup} \sigma_2 \dot{\cup} \dots \dot{\cup} \sigma_r,$$

where $(i \in \sigma_k \text{ and } j \in \sigma_l)$ implies $(\ell_i = \ell_j \text{ if and only if } k = l)$. We write $\ell_{\sigma_k}(t)$ for the linear function $\ell_i(t)$ with $i \in \sigma_k$. The tropical polynomial function $\mathbb{R} \rightarrow \mathbb{R}^{m+1}$, $t \mapsto \min \ell(t)$ defines a partition into smaller intervals,

$$(8) \quad U = U_1 \cup U_2 \cup \dots \cup U_s,$$

with the following property: on each U_i precisely one function $\ell_{\sigma_{k(i)}}$ attains the minimum among our r linear functions. Then $\ell(t)$ covers U if and only if

$$(9) \quad |\sigma_{k(i)}| \geq 2 \quad \text{for all } i \in \{1, 2, \dots, s\}.$$

Our discussion translates into an algorithm called the *Covering Subroutine*. Its input is an interval U in \mathbb{R} and a list $\ell(t)$ of linear polynomials, and its output is a yes-no decision whether U is covered by $\ell(t)$. In the no-case, the Covering Subroutine also outputs a rational number $u \in U$ such that the minimum in $\ell(u)$ is attained only once. In the yes-case, the Covering Subroutine outputs the list of index sets $\sigma_{k(1)}, \sigma_{k(2)}, \dots, \sigma_{k(s)}$, along with the corresponding tropical roots of $\min \ell(t)$. We call this list the *covering certificate*.

We next present an algorithm that decides whether a given non-degenerate tropical line lies on a given tropical cubic surface. It makes five calls to the Covering Subroutine. An illustration of Algorithm 1 is given in Example 3.3.

Example 3.3. Fix the line L with $P = (26, 6, 17, 7, 18, 0)$ and the cubic F with

$$(10) \quad C = (32, 17, 20, 41, 26, 17, 32, 33, 36, 54, 8, 1, 14, 4, 7, 18, 0, 0, 0, 0).$$

This vector induces the honeycomb triangulation #12369387 from [22, §6]:

$$\begin{aligned} &\{0, 1, 4, 10\}, \{1, 2, 5, 11\}, \{1, 4, 5, 13\}, \{1, 4, 10, 13\}, \{1, 5, 11, 13\}, \{1, 10, 11, 13\}, \\ &\{2, 3, 6, 12\}, \{2, 5, 6, 14\}, \{2, 5, 11, 14\}, \{2, 6, 12, 14\}, \{2, 11, 12, 14\}, \{4, 5, 7, 13\}, \\ &\{5, 6, 8, 14\}, \{5, 7, 8, 15\}, \{5, 7, 13, 15\}, \{5, 8, 14, 15\}, \{5, 11, 13, 14\}, \{5, 13, 14, 15\}, \\ &\{7, 8, 9, 15\}, \{10, 11, 13, 16\}, \{11, 12, 14, 17\}, \{11, 13, 14, 18\}, \{11, 13, 16, 18\}, \\ &\{11, 14, 17, 18\}, \{11, 16, 17, 18\}, \{13, 14, 15, 18\}, \{16, 17, 18, 19\}. \end{aligned}$$

The tropical line L is non-degenerate and of labeled type 01|23 because $P_{02} + P_{13} = P_{03} + P_{12} = 24 < 26 = P_{01} + P_{23}$. Using (5) we find $q_{01} = (19, 20, 0, 11)$ and $q_{23} = (17, 18, 0, 11)$. In all five

Algorithm 1 Deciding if a tropical line L lies on a tropical surface S in \mathbb{R}^3

Input: The tropical Plücker vector P for L , and a tropical polynomial F that defines S .

Output: Either a certificate that L lies in S , or a point in the set difference $L \setminus S$.

- 1: Determine the labeled type $ij|kl$ of L
 - 2: Compute the vertices q_{ij} and q_{kl} of L via the formulas in (5)
 - 3: Find parametrizations for the bounded edge and the four rays of L . These are linear maps:
 $[0, 1] \rightarrow [q_{ij}, q_{kl}]$ and $[0, \infty) \rightarrow q_{ij} + \mathbb{R}_{\geq 0} \cdot \omega_i$ and \dots and $[0, \infty) \rightarrow q_{kl} + \mathbb{R}_{\geq 0} \cdot \omega_l$.
 - 4: **for** each of the five linear maps above **do**
 - 5: Substitute the map into F . Get an interval U and a list $\ell(t)$ of linear polynomials.
 - 6: Apply the Covering Subroutine to $(U, \ell(t))$ and obtain the answer yes or no.
 - 7: **if** no **then** obtain $u \in U$, plug into linear map, and output resulting point in $L \setminus S$.
 - 8: **end if**
 - 9: **if** yes **then** obtain the covering certificate $(\sigma_{k(1)}, \sigma_{k(2)}, \dots, \sigma_{k(s)})$ and save it.
 - 10: **end if**
 - 11: **end for**
 - 12: **if** all five answers were yes **then**
 - 13: Output the covering certificates for the bounded edge and the four rays of L .
 - 14: **end if**
-

iterations through steps 4–11, the answer is yes. The covering certificates σ are:

$$\begin{array}{llll}
 [q_{01}, q_{23}] & \text{has} & s = 1 \text{ and } \sigma = (\{14, 15\}) \\
 q_{01} + \mathbb{R}_{\geq 0}\omega_0 & \text{has} & s = 1 \text{ and } \sigma = (\{14, 15\}) \\
 (11) \quad q_{01} + \mathbb{R}_{\geq 0}\omega_1 & \text{has} & s = 2 \text{ and } \sigma = (\{14, 15\}, \{5, 8\}) \\
 q_{23} + \mathbb{R}_{\geq 0}\omega_2 & \text{has} & s = 2 \text{ and } \sigma = (\{14, 18\}, \{11, 17\}) \\
 q_{23} + \mathbb{R}_{\geq 0}\omega_3 & \text{has} & s = 1 \text{ and } \sigma = (\{15, 18\})
 \end{array}$$

There are two special points where $\min \ell(t)$ is attained four times. At the point q_{23} , the minimum is attained thrice. The relevant index sets are cells in the triangulation: two tetrahedra $\{5, 8, 14, 15\}$ and $\{11, 14, 17, 18\}$, and the triangle $\{14, 15, 18\}$. These data identify an occurrence of the motif 3D in Table 1.

Remark 3.4. Algorithm 1 can be turned into a method for identifying all non-degenerate tropical lines in a given tropical surface S in \mathbb{R}^3 . Here is an alternative method for the same task. Let F be the tropical polynomial defining S . First we compute the *dome* $\{(x, y) : x \in \mathbb{R}^3, y \leq F(x)\}$. This is an unbounded polyhedron in \mathbb{R}^4 which represents F . We obtain a description of the surface S as a polyhedral complex by projecting the codimension 2 skeleton of the dome. The maximal cells of S are obtained by a convex hull computation [14, §3]. From this we enumerate the poset of all cells of S ; cf. [15, Algorithm 1]. Each pair of cells is a candidate for possible locations of the two vertices q_{ij} and q_{kl} . These points are described as convex combinations of the cells' vertices with unknown coefficients. Whether or not they form the two vertices of a tropical line in S can be decided by checking the feasibility of a linear program.

Simon Hampe implemented a similar approach for tropical cubic surfaces. This is the function `lines_in_cubic` in the `polymake` extension `a-tint` [13], which is slightly different

from our Algorithm 1. First, `lines_in_cubic` also computes degenerate lines; second, that function is tailored to the cubic case.

4. MOTIFS AND THEIR OCCURRENCES

We now turn to the ten motifs in Table 1. We are interested in their occurrences in the 14 373 645 unimodular regular triangulations of $3\Delta_3$. As before, our goal is the complete classification of all possibilities. We begin by stating our main result. The proof is given by exhaustive computations using Algorithm 2.

Theorem 4.1. *The number of occurrences of all motifs in the unimodular regular triangulations of $3\Delta_3$ varies between 27 and 128, as shown in Figure 2. There are no triangulations with precisely 122, 124, 125 or 127 occurrences.*

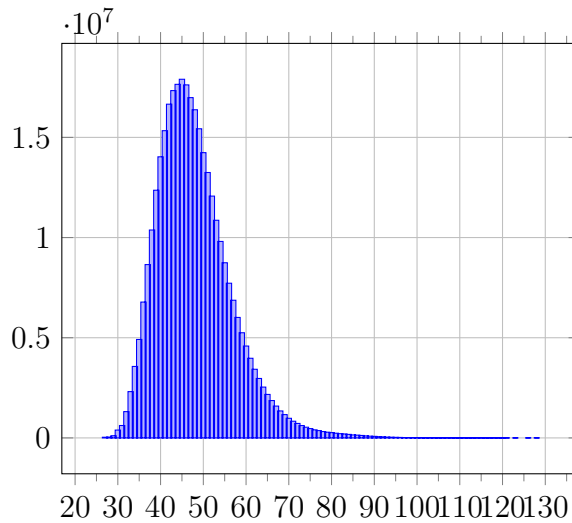


FIGURE 2. The distributions of the total number of motifs, counting triangulations. The highest frequency is 45 motifs, which occur in 17 900 688 triangulations. These form 745 927 orbits, which is 5.12% of orbits of regular unimodular triangulations of $3\Delta_3$. The minimum at 27 is attained by 34 096 triangulations in 1426 orbits, and the maximum at 128 by 15 triangulations in two orbits.

We now define the notion of occurrence. Fix a regular unimodular triangulation T of $3\Delta_3$. Let \mathcal{R} be a motif, viewed as a labeled simplicial complex. An *occurrence* of \mathcal{R} in T is a simplicial map from \mathcal{R} to T that satisfies the conditions in the third column of Table 1. These conditions include a bijection between the set $\{i, j, k, l\}$ of exits and the four facets of $3\Delta_3$. Such a *simplicial map* sends vertices of \mathcal{R} to vertices of T , while faces are mapped to faces. Often occurrences are embeddings, but it can happen that two vertices of \mathcal{R} are mapped to the same vertex of T . We shall see this in Example 4.4.

An occurrence of a motif \mathcal{R} in T is a map of simplicial complexes. The definition above is subtle. One might think that such a map is determined by the image of the set of vertices of \mathcal{R} . This is not true! The same subcomplex of T may support several occurrences of a motif. We now present an example.

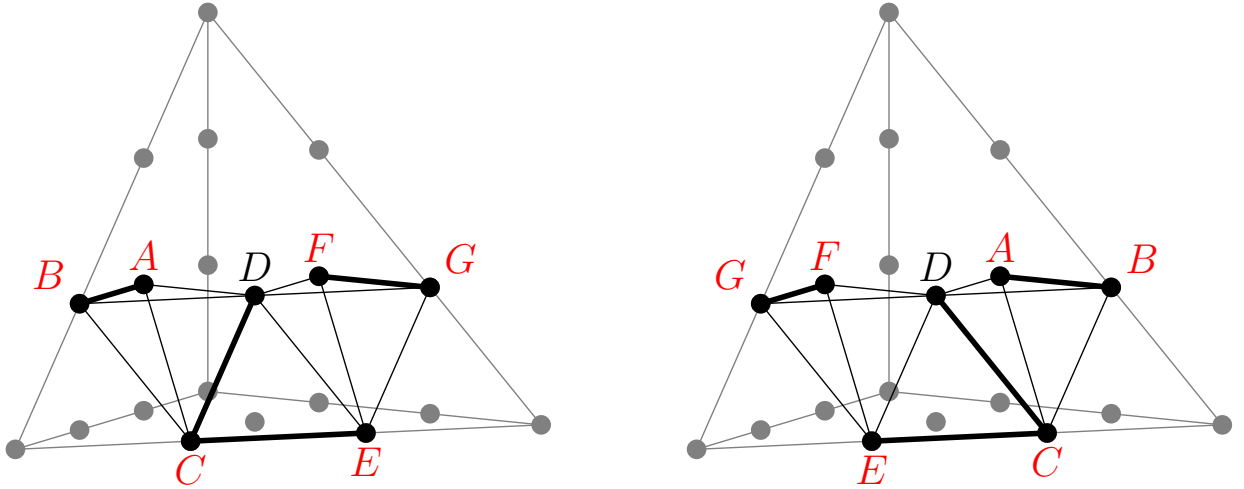


FIGURE 3. Two distinct 3D motifs in the honeycomb triangulation that are supported by the same set of vertices (cf. Example 4.2). Exit edges are marked.

Example 4.2. The line L in Example 3.3 gives an occurrence of the motif 3D in the honeycomb triangulation. The corresponding simplicial map is given by

$$(12) \quad \begin{aligned} A = 11, B = 17, C = 18, D = 14, E = 15, F = 5, G = 8, \\ i = 3, j = 2, k = 0, l = 1. \end{aligned}$$

This uses our fixed ordering of the lattice points in $3\Delta_3$, so the vertices are

$$A = (1101), B = (0201), C = (0210), D = (0111), E = (0120), F = (1011), G = (0021).$$

The left diagram in Figure 3 helps in verifying the conditions from Table 1:

$$CE \subset F_3, AB \subset F_2, DE \subset F_0, FG \subset F_1, CD \subset \{x_2 = 1\}, DE \subset \{x_1 = 1\}.$$

The motif (12) is made visible in Example 3.3 by the line L in the surface S . The motif occurrence is seen in the covering certificates (11) given by Algorithm 1.

The above occurrence is special in that the exit edge $\{15, 18\}$ lies in the edge $F_0 \cap F_3$ of $3\Delta_3$. We can relabel the points and the exits as follows:

$$\begin{aligned} A = 5, B = 8, C = 15, D = 14, E = 18, F = 11, G = 17, \\ i = 3, j = 1, k = 0, l = 2. \end{aligned}$$

This is another occurrence of a 3D motif in T , shown on the right in Figure 3.

In conclusion, the same subcomplex of the honeycomb triangulation supports two distinct occurrences of the motif 3D. However, it is impossible for both to be visible in the same cubic surface. To ascertain whether an occurrence of a motif is visible in a specific cubic surface is our problem in Section 5.

We now show all motif occurrences in a given triangulation. As it stands, Algorithm 2 is too naïve to be useful. The number of vertices of a motif varies between four (type 3I) and eight (type 3F). For the 3F motif alone we would need to enumerate and check $20^8 = 25.6 \cdot 10^9$ potential simplicial maps into T .

Algorithm 2 Finding all motif occurrences**Input:** Unimodular regular triangulation T of $3\Delta_3$.**Output:** The list of all occurrences of motifs in T .

```

1: for each motif  $M$  do
2:   for each map  $\mathcal{R}$  from the vertices of  $M$  to the 20 lattice points in  $3\Delta_3$  do
3:     if  $\mathcal{R}$  is simplicial into  $T$  and the conditions in Table 1 are satisfied then
4:       output  $\mathcal{R}$ .
5:     end if
6:   end for
7: end for

```

In practice, it is essential to exploit symmetries and other simplifications. A *symmetry* of a motif \mathcal{R} is a simplicial bijection from the labeled simplicial complex \mathcal{R} to itself such that the conditions in the third column of Table 1 are preserved. Two symmetric occurrences of a motif yield the same line in a given tropical surface (or none). The symmetries of a motif form a group. The following lemma is derived by direct inspection from the data in Table 1.

Lemma 4.3. *The ten motifs of tropical cubic surfaces have the following symmetry groups. In each case, generators g_1, g_2, \dots and a description are given:*

- (3A) $g_1 = (E\ F)$. Cyclic group of order 2.
- (3B) $g_1 = (B\ C)(i\ j)$, $g_2 = (A\ F)(B\ D)(C\ E)(i\ k)(j\ l)$. Dihedral group of order 8.
- (3C) $g_1 = (B\ C)(i\ j)$, $g_2 = (D\ E)$, $g_3 = (F\ G)$. Elementary abelian group of order 8.
- (3D) $g_1 = (A\ B)$, $g_2 = (F\ G)$. Elementary abelian group of order 4.
- (3E) $g_1 = (B\ C)(i\ j)$, $g_2 = (D\ E)$, $g_3 = (B\ C)(D\ F)(E\ G)(i\ j)(k\ l)$. Nonabelian group of order 16: direct product of an order 2 group $\langle g_1 \rangle$ and a dihedral group $\langle g_2, g_3 \rangle$ of order 8.
- (3F) $g_1 = (A\ B)$, $g_2 = (C\ D)$, $g_3 = (E\ F)$, $g_4 = (G\ H)$, $g_5 = (A\ H)(B\ G)(C\ F)(D\ E)(i\ k)(j\ l)$. Nonabelian group of order 32. Here g_1, g_2, g_3, g_4 span an abelian subgroup of order 16.
- (3G) $g_1 = (A\ B)$, $g_2 = (C\ D)$, $g_3 = (E\ F)$. Elementary abelian group of order 8.
- (3H) $g_1 = (A\ B)$, $g_2 = (C\ D)(k\ l)$. Elementary abelian group of order 4.
- (3I) $g_1 = (A\ B)$, $g_2 = (C\ D)$. Elementary abelian group of order 4.
- (3J) $g_1 = (B\ C)$, $g_2 = (D\ E)$. Elementary abelian group of order 4.

We next show that occurrences of motifs are generally not embeddings.

Example 4.4. The motif 3F occurs in the triangulation (3) via the labeling

$$A = 15, B = 18, C = 11, D = 17, E = 14, F = 15, G = 2, H = 9, i = 2, j = 3, k = 0, l = 1.$$

In this occurrence, A and F are mapped to the same point, labeled by 15.

To obtain Theorem 4.1, we developed a highly efficient version of Algorithm 2, we implemented it in `polymake`, and we applied it to millions of triangulations. This required substantial speed-ups, based on structural constraints that control the combinatorial explosion. In the rest of this section, we present a sample of such constraints, and we discuss how they are used.

Lemma 4.5. *Vertex A is distinct from E and F in any occurrence of motif 3A.*

Proof. If A coincides with E or F then A has coordinates i, k and l equal to zero. Moreover, the condition $AD \subseteq \{x_i + x_j = 1\}$ implies that the coordinate j is equal to one. This is impossible, since the four coordinates sum to three. \square

Our strategy for enumerating motif occurrences is to find the possible ways in which the simplices of a motif are mapped into the given triangulation. This leads to more book-keeping in Algorithm 2, to be used for shortcuts. We exploit the following features in the various motifs. A tetrahedron T is called *sided* if it has one edge on a facet F_i of $3\Delta_3$ and the opposite edge lies on the plane $x_i = 1$. The associated tropical line contains the vertex of the surface dual to T in the interior of the ray in direction ω_i . We call T *split* if it has two opposite edges with prescribed exits. Here there are two possibilities. The line has two adjacent rays in directions given by the exits, and one ray contains in its interior the vertex dual to the split tetrahedron. Or the bounded edge contains the vertex dual to the split tetrahedron in its interior, and the rays in directions given by the exits are not adjacent. We say that T is *centered* if the constraints in Table 1 induce a bijection between its vertices and the facets of $3\Delta_3$. Its dual vertex lies in the interior of the bounded edge of the tropical line. Finally, a triangle in a motif is *dangling* if it has two edges with required exits. The tropical line has a vertex in the interior of an edge of the surface. The two rays adjacent to that vertex have direction given by the exits of the dangling triangle.

The features we defined above occur in the ten motifs as follows:

- The following tetrahedra are sided: $CDEF$ in motif 3A, $DEFG$ in 3C, $BCDE$ and $BCFG$ in 3E, $ABCD$ and $EFGH$ in 3F, $CDEF$ in 3G, $ABCD$ and $ABCE$ in 3J.
- Tetrahedron $DEFG$ in 3D is split; so are $CDEF$ in 3F and $CDEF$ in 3G.
- Tetrahedron $BCDE$ in motif 3B is centered.
- Triangle ABD in motif 3A is dangling, likewise ABC and DEF in 3B, ABC in 3C, CDE in 3D, ABC in 3E, and CDE in 3H.

Our strategy for Theorem 4.1 is to first enumerate the features of a triangulation, i.e. its sided, split and centered tetrahedra, and its dangling triangles. This is combined with searching for occurrences of a motif by local extensions.

We illustrate this for the 3A motif with a heuristic estimate for the number of subcases arising. Let T be the triangulation in (3) and in Example 5.3 below. We start out by finding the candidates for the sided tetrahedron $CDEF$, with the exit EF on facet F_l . Considering all labelings, there are 114 choices for this in T . Next we need to find the candidates for A . Here it suffices to consider those which are in the link of the edge CD . For instance, the link for $\{C, D\} = \{15, 11\}$ has six vertices. The number six appears to be typical and we use this number for our estimate. By Lemma 4.5, A must be distinct from E and F , reducing the number of candidates to four. We further exclude any A where AC does not lie in the boundary of $3\Delta_3$. For the remaining ones we try the three directions other than l , which is already fixed. The only item missing is the vertex B . Assuming, e.g., $A = 18$ we need to check three candidates in the link of AD (four minus one for C , because $A \neq C$) and two remaining exits. This leads to $114 \cdot 4 \cdot 3 \cdot 3 \cdot 2 = 8208$ cases, including all possible labelings. In fact, the enumeration is even faster, as many of these cases can be ruled out early while the various conditions in Table 1 are being checked. Summing up, the number of subcases considered by this approach is much smaller than 3.3 million subcases for one 3A motif one sees in a naïve backtracking search.

5. SCHLÄFLI CONES

In Section 4 we studied the occurrences of motifs in the 14 373 645 types of regular unimodular triangulations of $3\Delta_3$. Their number per type ranges between 27 and 128. In this section we focus on individual smooth tropical cubic surfaces from a fixed secondary cone $\text{sec}(T)$. Every tropical line on a generic surface gives a motif that occurs in T . But the converse is not true. An occurrence of a motif need not contribute a tropical line to a given surface.

Let T be a regular unimodular triangulation of $3\Delta_3$. Each point C in the open secondary cone $\text{sec}(T)$ specifies a smooth tropical cubic surface S_C which is dual to the triangulation T . Given an occurrence \mathcal{R} of a motif in T , we say that \mathcal{R} is *visible in S_C* if there is a tropical line L in S_C that has the dual complex \mathcal{R} . We write \mathcal{M}_C for the set of all motifs that are visible in S_C .

We regard two vectors C and C' in $\text{sec}(T)$ as *equivalent* if $\mathcal{M}_C = \mathcal{M}_{C'}$. Each equivalence class is a finite union of relatively open convex polyhedral cones in \mathbb{R}^{20} . The full-dimensional cones among these are the *Schläfli cones*. Each facet of a Schläfli cone is defined by a linear form in $\mathbb{Z}[c_0, c_1, \dots, c_{19}]$. This linear form is unique up to scaling. We identify this linear form with the hyperplane it defines, and we call it a *Schläfli wall* for the type T . The collection of all Schläfli walls defines a hyperplane arrangement in \mathbb{R}^{20} .

The *Schläfli fan* of the combinatorial type T is the subdivision of $\text{sec}(T)$ induced by the Schläfli walls of type T . Every maximal cone of the Schläfli fan is fully contained in a Schläfli cone. Hence, the set \mathcal{M}_C is constant for all surfaces S_C in a fixed maximal cone of the Schläfli fan. A tropical cubic surface S_C is *generic* if its coefficient vector C is in the interior of a Schläfli cone. Notice that, in general, a Schläfli cones need not be a cone of the Schläfli fan.

There are 14 373 645 distinct Schläfli fans. Algorithm 3 finds their Schläfli walls. We coded this in Macaulay2 [12]. Here is one of the results we found:

Theorem 5.1. *For each of the 1426 types in Theorem 4.1 with exactly 27 motifs, the secondary cone remains undivided in the Schläfli fan. Among these, 1396 types feature isolated tropical lines only. The remaining 30 have precisely one occurrence of motif 3I; in particular, motif 3J does not occur at all.*

The situation is different for many triangulations T with more than 27 motif occurrences. Here, the Schläfli fan is nontrivial; it does divide $\text{sec}(T)$ into smaller cones, according to which tropical lines lie on the various cubic surfaces. Each Schläfli wall arises (non-uniquely) from some motif \mathcal{R} that occurs in T . If one crosses from one Schläfli cone to a neighboring one through a shared facet, then the set \mathcal{M}_C of visible motifs changes. If a motif \mathcal{R} is no longer visible then the Schläfli wall gives a linear inequality that is necessary for \mathcal{R} to be visible. We write $\mathcal{W}_{\mathcal{R}}$ for the set of Schläfli walls arising from the motif \mathcal{R} .

Lemma 5.2. *Let \mathcal{R} be an occurrence of a motif 3F, 3G or 3I in a type T . Then $\mathcal{W}_{\mathcal{R}} = \emptyset$. In other words, \mathcal{R} is visible in every tropical cubic surface of type T .*

Proof. This was shown for the motifs 3G and 3I in [22, Proposition 23]. Now consider the motif 3F. Suppose that \mathcal{R} is an occurrence of 3F. The three tetrahedra $ABCD$, $CDEF$ and $EFGH$ are dual to three vertices of S_C . The necessary conditions on the edges in Table 1 allow trespassing segments respectively in the directions ω_j , $\omega_i + \omega_j$ and ω_l . Thanks to the exits of the three tetrahedra, these segments can always be completed to a tropical line, irrespective of the specific values of the parameters c_i . \square

We now discuss how the set of walls $\mathcal{W}_{\mathcal{R}}$ can be computed for the other motifs. The basic idea is this. Given \mathcal{R} , we compute a tropical line that matches the combinatorics in \mathcal{R} . The line is uniquely determined by its two vertices. Their coordinates are linear forms in $C = (c_0, c_1, \dots, c_{19})$. In this section we use lowercase letters c_i instead of uppercase letters C_i for the coordinates of the tropical coefficient vector C , so as to make our tables more readable.

Algorithm 3 Computing the visibility cone and Schläfli walls of a motif

Input: Secondary cone of a unimodular regular triangulation T of $3\Delta_3$, and an occurrence \mathcal{R} of a motif in T

Output: Visibility cone and Schläfli walls of \mathcal{R}

- 1: Compute the vertices of the tropical line L dual to \mathcal{R} .
 - 2: **for each** vertex V of L **do**
 - 3: Substitute the coordinates of V in the 20 monomials of the tropical cubic polynomial.
 - 4: Get linear inequalities by requiring that V lies on the prescribed cell of the surface.
 - 5: **end for**
 - 6: Construct the cone defined by these linear inequalities.
 - 7: Compute the visibility cone by intersecting that cone with the secondary cone.
 - 8: Remove redundant facets.
 - 9: Output the visibility cone and Schläfli walls.
-

If the c_i take on values in \mathbb{R} then the tropical line may or may not be contained in S_C . We require that it lies in S_C as prescribed by \mathcal{R} . Each vertex must lie on a cell of S_C that is specified by the tropical cubic polynomial. These linear forms must be equal and bounded above by the other ones. We consider these linear inequalities together with those that define the secondary cone. They define the *visibility cone* of \mathcal{R} in $\sec(T)$. The irredundant linear inequalities for this cone give us the linear forms in $\mathcal{W}_{\mathcal{R}}$. A Schläfli cone is the intersection of the full dimensional visibility cones of the visible motifs.

If all linear inequalities we found are redundant, then the visibility cone equals the secondary cone. In that case, the motif is visible in each surface S_C with $C \in \sec(T)$, and the motif is *globally visible*. This holds in Theorem 5.1.

If Algorithm 3 finds irredundant linear forms, then we distinguish two cases, according to the dimension of the visibility cone. If the visibility cone is full dimensional, then the motif is *partially visible*. Finally, a visibility cone might not be full dimensional. This means that it is contained in a linear space of positive codimension. A motif with visibility cone of lower dimension is not visible in generic surfaces. We therefore call it *hardly visible*.

We now illustrate these concepts for the tropical cubic surface from (3).

Example 5.3. The triangulation #5054117 has 51 occurrences of the motifs 3A, 3B, \dots , 3J. Their frequencies are 6, 5, 0, 24, 0, 2, 4, 7, 2, 1. Lemma 5.2 says that the motifs 3F, 3G and 3I are globally visible. In Tables 4, 5 and 6 we list all motifs, together with their sets of Schläfli walls $\mathcal{W}_{\mathcal{R}}$. We describe how the Schläfli walls are computed for the motifs of type 3H. The motif \mathcal{R} consists of a tetrahedron $ABCD$ and a dangling triangle CDE . One of the vertices of the tropical line defined by \mathcal{R} is dual to the tetrahedron. In order for the line to be contained in the surface, the other vertex must lie on the edge dual to the dangling triangle, i.e., the minimum in the tropical polynomial must be achieved at the monomials corresponding to C ,

TABLE 4. The triangulation #5054117 from (3) has 24 globally visible motifs.

Index	Points	Exits
Motifs 3B		
0	9, 15, 7, 1, 18, 19	0, 1, 2, 3
Motifs 3D		
1	9, 15, 2, 11, 1, 9, 15	1, 0, 2, 3
2	3, 14, 2, 11, 1, 15, 18	1, 0, 2, 3
3	9, 15, 2, 11, 1, 15, 18	1, 0, 2, 3
4	14, 15, 2, 11, 1, 15, 18	1, 0, 2, 3
5	3, 14, 2, 11, 1, 18, 19	1, 0, 2, 3
6	9, 15, 2, 11, 1, 18, 19	1, 0, 2, 3
7	14, 15, 2, 11, 1, 18, 19	1, 0, 2, 3
8	9, 15, 1, 11, 2, 3, 14	1, 3, 2, 0
9	9, 15, 1, 11, 2, 14, 15	1, 3, 2, 0
10	9, 15, 1, 11, 2, 9, 15	1, 3, 2, 0
11	2, 3, 14, 11, 17, 15, 18	0, 1, 2, 3
12	2, 3, 14, 11, 17, 18, 19	0, 1, 2, 3
Motifs 3F		
13	15, 18, 11, 17, 14, 15, 2, 9	2, 3, 0, 1
14	18, 19, 11, 17, 14, 15, 2, 9	2, 3, 0, 1
Motifs 3G		
15	9, 15, 2, 11, 3, 14	1, 3, 2, 0
16	9, 15, 2, 11, 14, 15	1, 3, 2, 0
17	9, 15, 1, 11, 15, 18	0, 1, 2, 3
18	9, 15, 1, 11, 18, 19	0, 1, 2, 3
Motifs 3H		
19	7, 15, 1, 18, 19	0, 1, 2, 3
20	9, 15, 2, 14, 3	1, 3, 2, 0
Motifs 3I		
21	1, 11, 9, 15	1, 2, 0, 3
22	2, 11, 9, 15	1, 2, 0, 3
Motifs 3J		
23	11, 9, 15, 1, 2	0, 3, 1, 2

D and E . These linear inequalities define the visibility cone. Note that the occurrence 8 of motif 3H in Table 6 is hardly visible, since its visibility cone is not full dimensional.

The list of partially visible motifs in Table 5 shows that the Schläfli walls generate a hyperplane arrangement defined by the seven linear forms:

$$\begin{aligned}
H_0 &: c_2 - c_9 - c_{11} + c_{15} - c_{17} + c_{18} \\
H_1 &: c_2 - c_9 - c_{11} + 2c_{15} - c_{17} - c_{18} + c_{19} \\
H_2 &: c_1 - c_9 - 2c_{11} + 2c_{15} + c_{17} - c_{18} \\
H_3 &: c_1 - c_9 - 2c_{11} + c_{15} + c_{17} + c_{18} - c_{19} \\
H_4 &: c_1 - c_7 + c_9 - c_{11} - c_{15} + c_{18} \\
H_5 &: c_1 - 2c_{11} - c_{15} + c_{17} + 2c_{18} - c_{19} \\
H_6 &: c_4 - c_7 - c_{13} + 2c_{18} - c_{19}
\end{aligned}$$

We write H_i^+ and H_i^- for the two halfspaces defined by these linear forms.

TABLE 5. The triangulation #5054117 from (3) has 18 partially visible motifs.

Index	Points	Exits	Schläfli walls
Motifs 3A			
0	18, 17, 15, 11, 2, 9	0, 2, 3, 1	$-c_2 + c_9 + c_{11} - c_{15} + c_{17} - c_{18},$ $c_2 - c_9 - c_{11} + 2c_{15} - c_{17} - c_{18} + c_{19}$
1	18, 19, 15, 11, 2, 9	3, 2, 0, 1	$-c_2 + c_9 + c_{11} - c_{15} + c_{17} - c_{18}$
2	18, 19, 15, 11, 2, 9	0, 2, 3, 1	$-c_2 + c_9 + c_{11} - 2c_{15} + c_{17} + c_{18} - c_{19}$
3	18, 17, 15, 11, 1, 9	0, 2, 3, 1	$c_1 - c_9 - 2c_{11} + 2c_{15} + c_{17} - c_{18},$ $-c_1 + c_9 + 2c_{11} - c_{15} - c_{17} - c_{18} + c_{19}$
4	18, 19, 15, 11, 1, 9	3, 2, 0, 1	$c_1 - c_9 - 2c_{11} + 2c_{15} + c_{17} - c_{18}$
5	18, 19, 15, 11, 1, 9	0, 2, 3, 1	$c_1 - c_9 - 2c_{11} + c_{15} + c_{17} + c_{18} - c_{19}$
Motifs 3B			
6	17, 18, 11, 1, 15, 7	0, 2, 1, 3	$c_1 - c_7 + c_9 - c_{11} - c_{15} + c_{18},$ $-c_1 + 2c_{11} + c_{15} - c_{17} - 2c_{18} + c_{19}$
7	17, 18, 11, 1, 15, 9	0, 2, 1, 3	$-c_1 + c_7 - c_9 + c_{11} + c_{15} - c_{18},$ $-c_1 + 2c_{11} + c_{15} - c_{17} - 2c_{18} + c_{19}$
8	19, 18, 11, 1, 15, 7	0, 2, 1, 3	$c_1 - c_7 + c_9 - c_{11} - c_{15} + c_{18},$ $c_1 - 2c_{11} - c_{15} + c_{17} + 2c_{18} - c_{19}$
9	19, 18, 11, 1, 15, 9	0, 2, 1, 3	$-c_1 + c_7 - c_9 + c_{11} + c_{15} - c_{18},$ $c_1 - 2c_{11} - c_{15} + c_{17} + 2c_{18} - c_{19}$
Motifs 3D			
10	1, 9, 15, 11, 17, 15, 18	0, 1, 2, 3	$-c_1 + c_9 + 2c_{11} - 2c_{15} - c_{17} + c_{18}$
11	2, 9, 15, 11, 17, 15, 18	0, 1, 2, 3	$c_2 - c_9 - c_{11} + c_{15} - c_{17} + c_{18}$
12	1, 9, 15, 11, 17, 18, 19	0, 1, 2, 3	$-c_1 + c_9 + 2c_{11} - 2c_{15} - c_{17} + c_{18}$
13	2, 9, 15, 11, 17, 18, 19	0, 1, 2, 3	$c_2 - c_9 - c_{11} + c_{15} - c_{17} + c_{18}$
Motifs 3H			
14	18, 19, 1, 13, 4	0, 2, 1, 3	$-c_4 + c_7 + c_{13} - 2c_{18} + c_{19}$
15	11, 18, 1, 15, 9	0, 2, 1, 3	$-c_1 + c_7 - c_9 + c_{11} + c_{15} - c_{18}$
16	18, 19, 1, 13, 7	0, 2, 1, 3	$c_4 - c_7 - c_{13} + 2c_{18} - c_{19}$
17	11, 18, 1, 15, 7	0, 2, 1, 3	$c_1 - c_7 + c_9 - c_{11} - c_{15} + c_{18}$

Let us look at the Schläfli walls from partially visible motifs of type 3B. The hyperplanes for the Schläfli walls of these motifs are H_4 and H_5 . They divide the secondary cone into four cells $H_4^+ H_5^+$, $H_4^+ H_5^-$, $H_4^- H_5^+$, $H_4^- H_5^-$. These four cells correspond in Table 5 to the occurrences 8, 6, 7 and 9, in this order. Each motif occurrence is visible in precisely that cell.

For the motifs of type 3D, we also have two hyperplanes H_0 and H_2 . These give the Schläfli walls that divide the secondary cone into four cells. In the cells $H_0^+ H_2^+$ and $H_0^- H_2^-$ the motifs 11, 13 and 10, 12 are visible, respectively. In the cell $H_0^- H_2^+$ none of the partially visible motif is visible. Finally, on the cell $H_0^+ H_2^-$ all the partially visible motifs are visible. Moreover, when we pass through the Schläfli wall from H_0^- to H_0^+ , the motifs 0 and 1 of type 3A are no longer visible, while the motifs 11 and 13 of type 3D become visible.

Remark 5.4. In this section we have considered the problem whether a motif is visible on a certain tropical surface. If the motif is visible, the next natural step is to ask whether the tropical line defined by the motif is realizable on a cubic surface defined over a field with valuation. More precisely, given a tropical line L on a tropical surface S , we ask whether there exists a line ℓ on a cubic surface \mathcal{S} such that $\text{trop}(\ell) = L$ and $\text{trop}(\mathcal{S}) = S$. This

TABLE 6. The triangulation #5054117 from (3) has 9 hardly visible motifs.

Index	Points	Exits	Schläfli walls
Motifs 3D			
0	3, 14, 2, 11, 1, 9, 15	1, 0, 2, 3	$c_{12} - 2c_{14} + c_{15},$ $c_1 - 3c_5 + 2c_9 + c_{11} + c_{14} - 2c_{15},$ $c_9 - 2c_{12} + 3c_{14} - 3c_{15} + c_{17},$ $c_3 - 2c_6 + c_8, \quad -c_3 + 2c_6 - c_8$ Equations: $c_2 - c_6 - c_{11} + c_{14},$ $2c_3 - 3c_6 + c_9, \quad c_2 + c_3 - 2c_6 - c_{11} + c_{15}$
1	14, 15, 2, 11, 1, 9, 15	1, 0, 2, 3	$c_1 - 3c_5 + 2c_9 + c_{11} + c_{14} - 2c_{15},$ $-c_3 + c_9 + c_{12} + c_{14} - 2c_{15}$ Equation: $c_2 - c_9 - c_{11} - c_{14} + 2c_{15}$ $-2c_6 + c_8 + 2c_{12} - c_{17}, \quad c_8 - c_9 - c_{17} + c_{18},$ $c_1 - 3c_5 + c_9 + c_{11} + c_{12} - c_{17},$ $c_9 - c_{12} - c_{15} + 2c_{17} - c_{18},$ Equations:
2	15, 18, 1, 11, 2, 3, 14	1, 3, 2, 0	$c_2 - c_3 - c_{11} + c_{12}, \quad 2c_2 - c_3 - 2c_{11} + c_{17},$ $2c_2 - c_3 - 2c_{11} + c_{14} - c_{15} + c_{18}$ $-2c_6 + c_8 + 2c_{12} - c_{17},$ $c_1 - 3c_5 + c_9 + c_{11} + c_{12} - c_{17},$ $c_8 - c_9 - c_{17} + c_{18}, \quad -c_1 + c_{11} + c_{13} - c_{18},$ $c_9 - c_{12} + 2c_{17} - 3c_{18} + c_{19},$ $c_5 - c_9 - c_{11} + 2c_{18} - c_{19},$ Equations: $c_2 - c_3 - c_{11} + c_{12},$ $2c_2 - c_3 - c_7 - 2c_{11} + c_{13} + c_{14},$ $2c_2 - c_3 - 2c_{11} + c_{17}, \quad c_7 - c_{13} - c_{15} + c_{18},$ $2c_7 - 2c_{13} - c_{15} + c_{19}$
3	18, 19, 1, 11, 2, 3, 14	1, 3, 2, 0	$c_5 - c_{11} - c_{15} + c_{18},$ $c_1 - 3c_5 + c_{11} + 3c_{15} + c_{17} - 3c_{18}$ Equations: $c_3 - 2c_6 + c_8,$ $2c_3 - 3c_6 + c_9, \quad c_2 - c_3 - c_{11} + c_{12},$ $c_2 - c_6 - c_{11} + c_{14},$ $c_2 + c_3 - 2c_6 - c_{11} + c_{15},$ $2c_2 - c_3 - 2c_{11} + c_{17}, \quad 2c_2 - c_6 - 2c_{11} + c_{18}$ $-c_1 + c_{11} + c_{13} - c_{18}, \quad c_5 - c_{11} - c_{18} + c_{19},$ $c_1 - 3c_5 + c_{11} + c_{17} + 3c_{18} - 3c_{19}$ Equations: $c_3 - 2c_6 + c_8,$ $2c_3 - 3c_6 + c_9, \quad c_2 - c_3 - c_{11} + c_{12},$ $c_2 - c_3 + c_6 - c_7 - c_{11} + c_{13},$ $c_2 + c_3 - 2c_6 - c_{11} + c_{15},$ $c_2 - c_6 - c_{11} + c_{14}, \quad 2c_2 - c_3 - 2c_{11} + c_{17},$ $2c_2 - c_6 - 2c_{11} + c_{18}, \quad 3c_2 - c_3 - 3c_{11} + c_{19}$
4	15, 18, 1, 11, 2, 9, 15	1, 3, 2, 0	$c_5 - c_{11} - c_{15} + c_{18},$ $c_1 - 3c_5 + c_{11} + 3c_{15} + c_{17} - 3c_{18}$ Equations: $c_3 - 2c_6 + c_8,$ $2c_3 - 3c_6 + c_9, \quad c_2 - c_3 - c_{11} + c_{12},$ $c_2 - c_6 - c_{11} + c_{14},$ $c_2 + c_3 - 2c_6 - c_{11} + c_{15},$ $2c_2 - c_3 - 2c_{11} + c_{17}, \quad 2c_2 - c_6 - 2c_{11} + c_{18}$ $-c_1 + c_{11} + c_{13} - c_{18}, \quad c_5 - c_{11} - c_{18} + c_{19},$ $c_1 - 3c_5 + c_{11} + c_{17} + 3c_{18} - 3c_{19}$ Equations: $c_3 - 2c_6 + c_8,$ $2c_3 - 3c_6 + c_9, \quad c_2 - c_3 - c_{11} + c_{12},$ $c_2 - c_3 + c_6 - c_7 - c_{11} + c_{13},$ $c_2 + c_3 - 2c_6 - c_{11} + c_{15},$ $c_2 - c_6 - c_{11} + c_{14}, \quad 2c_2 - c_3 - 2c_{11} + c_{17},$ $2c_2 - c_6 - 2c_{11} + c_{18}, \quad 3c_2 - c_3 - 3c_{11} + c_{19}$
5	18, 19, 1, 11, 2, 9, 15	1, 3, 2, 0	$c_5 - c_{11} - c_{15} + c_{18},$ $c_1 - 3c_5 + c_{11} + 3c_{15} + c_{17} - 3c_{18}$ Equations: $c_3 - 2c_6 + c_8,$ $2c_3 - 3c_6 + c_9, \quad c_2 - c_3 - c_{11} + c_{12},$ $c_2 - c_6 - c_{11} + c_{14}, \quad c_2 + c_3 - 2c_6 - c_{11} + c_{15},$ $2c_2 - c_3 - 2c_{11} + c_{17}, \quad 2c_2 - c_6 - 2c_{11} + c_{18}$ $-c_1 + c_{11} + c_{13} - c_{18}, \quad c_5 - c_{11} - c_{18} + c_{19}$ $c_1 - 3c_5 + c_{11} + c_{17} + 3c_{18} - 3c_{19}$ Equations: $c_3 - 2c_6 + c_8, \quad 2c_3 - 3c_6 + c_9,$ $c_2 - c_3 + c_6 - c_7 - c_{11} + c_{13},$ $c_2 - c_3 - c_{11} + c_{12}, \quad c_2 - c_6 - c_{11} + c_{14},$ $c_2 + c_3 - 2c_6 - c_{11} + c_{15}, \quad 2c_2 - c_3 - 2c_{11} + c_{17},$ $2c_2 - c_6 - 2c_{11} + c_{18}, \quad 3c_2 - c_3 - 3c_{11} + c_{19}$
6	15, 18, 1, 11, 2, 14, 15	1, 3, 2, 0	$c_5 - c_{11} - c_{15} + c_{18},$ $c_1 - 3c_5 + c_{11} + 3c_{15} + c_{17} - 3c_{18}$ Equations: $c_3 - 2c_6 + c_8,$ $2c_3 - 3c_6 + c_9, \quad c_2 - c_3 - c_{11} + c_{12},$ $c_2 - c_6 - c_{11} + c_{14}, \quad c_2 + c_3 - 2c_6 - c_{11} + c_{15},$ $2c_2 - c_3 - 2c_{11} + c_{17}, \quad 2c_2 - c_6 - 2c_{11} + c_{18}$ $-c_1 + c_{11} + c_{13} - c_{18}, \quad c_5 - c_{11} - c_{18} + c_{19}$ $c_1 - 3c_5 + c_{11} + c_{17} + 3c_{18} - 3c_{19}$ Equations: $c_3 - 2c_6 + c_8, \quad 2c_3 - 3c_6 + c_9,$ $c_2 - c_3 + c_6 - c_7 - c_{11} + c_{13},$ $c_2 - c_3 - c_{11} + c_{12}, \quad c_2 - c_6 - c_{11} + c_{14},$ $c_2 + c_3 - 2c_6 - c_{11} + c_{15}, \quad 2c_2 - c_3 - 2c_{11} + c_{17},$ $2c_2 - c_6 - 2c_{11} + c_{18}, \quad 3c_2 - c_3 - 3c_{11} + c_{19}$
7	18, 19, 1, 11, 2, 14, 15	1, 3, 2, 0	$c_5 - c_{11} - c_{15} + c_{18},$ $c_1 - 3c_5 + c_{11} + 3c_{15} + c_{17} - 3c_{18}$ Equations: $c_3 - 2c_6 + c_8, \quad 2c_3 - 3c_6 + c_9,$ $c_2 - c_3 + c_6 - c_7 - c_{11} + c_{13},$ $c_2 - c_3 - c_{11} + c_{12}, \quad c_2 - c_6 - c_{11} + c_{14},$ $c_2 + c_3 - 2c_6 - c_{11} + c_{15}, \quad 2c_2 - c_3 - 2c_{11} + c_{17},$ $2c_2 - c_6 - 2c_{11} + c_{18}, \quad 3c_2 - c_3 - 3c_{11} + c_{19}$
Motifs 3H			
8	9, 11, 1, 15, 7	0, 2, 1, 3	$c_2 - 3c_5 + c_7 + c_9 + c_{11} - c_{15},$ Equation: $c_1 - c_7 - c_{11} + c_{15}$

realizability problem has been studied in [2] and [3]. The authors show that non-degenerate lines in families of type 3I are not realizable on surfaces over a valued field of characteristic zero. Moreover, in the recent article [9] the result is extended to valued field with residue field of characteristic different from two. The paper also provides an example of a line of type 3J which is realizable on a cubic surface defined over the field of 5-adic numbers.

6. THE UNIVERSAL FANO VARIETY AND ITS TROPICAL DISCRIMINANT

We now relate our combinatorial results to classical algebraic geometry. The natural parameter space for our problem is the *universal Fano variety*. Its points are pairs consisting of a line and a cubic surface that contains it. The map onto the second factor is a 27-to-1 cover of \mathbb{P}^{19} . The fiber over a smooth cubic surface, regarded as a point in \mathbb{P}^{19} , is the *Fano variety* on that surface, i.e. the set of its 27 lines. The branch locus of the 27-to-1 map is its *discriminant*, a hypersurface in \mathbb{P}^{19} . We shall see that the codimension one skeleton of the Schläfli fan plays the role of the tropical discriminant for this map.

We follow the approach to tropical geometry in the textbook [18]. One starts with a classical variety, defined by an ideal I in a (Laurent) polynomial ring over a field with valuation. The tropical variety $\text{Trop}(I)$ is the set of all weight vectors w whose initial ideal $\text{in}_w(I)$ contains no monomials. We would like to apply this to the universal Fano variety for lines on cubic surfaces, represented by an ideal in the polynomial ring in the unknowns p_{ij} and c_k . This is the homogeneous coordinate ring of $\mathbb{P}^5 \times \mathbb{P}^{19}$. The first factor contains the Grassmannian $G(2, 4)$ of lines in \mathbb{P}^3 as a quadratic hypersurface in \mathbb{P}^5 .

The quadric defining $G(2, 4)$ is the Pfaffian of the skew-symmetric matrix

$$\mathcal{P} = \begin{pmatrix} 0 & p_{01} & p_{02} & p_{03} \\ -p_{01} & 0 & p_{12} & p_{13} \\ -p_{02} & -p_{12} & 0 & p_{23} \\ -p_{03} & -p_{13} & -p_{23} & 0 \end{pmatrix}.$$

We have $\text{Pfaff}(\mathcal{P}) = p_{01}p_{23} - p_{02}p_{13} + p_{03}p_{12}$. The line with Plücker coordinates (p_{ij}) is the image in \mathbb{P}^3 of the column span of the associated rank 2 matrix \mathcal{P} .

The second factor \mathbb{P}^{19} parametrizes cubic forms f . Its coordinates are the coefficients $(c_0, c_1, \dots, c_{19})$. Fix a row vector of unknowns $\lambda = (\lambda_0, \lambda_1, \lambda_2, \lambda_3)$ and form the vector-matrix product $\lambda\mathcal{P}$. We write $f(\lambda\mathcal{P})$ for the polynomial obtained by replacing (w, x, y, z) with $\lambda\mathcal{P}$. Thus, $f(\lambda\mathcal{P})$ is a homogeneous cubic in λ . Its 20 coefficients are bihomogeneous forms of degree $(3, 1)$, like

$$(13) \quad \begin{aligned} & p_{01}p_{12}p_{13}c_5 - p_{12}^2p_{13}c_8 + p_{01}p_{12}^2c_7 - p_{12}p_{13}^2c_6 - p_{12}^3c_9 \\ & + p_{01}p_{13}^2c_2 - p_{01}^2p_{12}c_4 - p_{01}^2p_{13}c_1 - p_{13}^3c_3 + p_{01}^3c_0. \end{aligned}$$

We write I_{ufv} for the ideal in $\mathbb{Q}[p_{01}, p_{02}, \dots, p_{23}, c_0, c_1, \dots, c_{19}]$ that is generated by these 20 polynomials together with the Plücker quadric $\text{Pfaff}(\mathcal{P})$.

The zero set of I_{ufv} in $\mathbb{P}^5 \times \mathbb{P}^{19}$ is the universal Fano variety of lines on cubic surfaces. We verified by computations on affine charts that the ideal I_{ufv} defines the correct scheme. We consider the *tropical universal Fano variety*

$$\text{Trop}(I_{\text{ufv}}) \subset \text{TP}^5 \times \text{TP}^{19}.$$

By the Structure Theorem [18, Theorem 3.3.5], $\text{Trop}(I_{\text{ufv}})$ is a pure 19-dimensional balanced fan. For simplicity, we disregard boundary phenomena, and we replace each tropical projective

space \mathbb{TP}^n with its dense tropical torus $\mathbb{R}^{n+1}/\mathbb{R}\mathbf{1}$. The former is compact while the latter is not. For a detailed discussion see [18, §6.2]. The points in $\text{Trop}(I_{\text{ufv}})$ are the pairs consisting of a line in \mathbb{TP}^3 and a cubic surface that contains the line. The tropical line is represented by its Plücker vector $P \in \mathbb{R}^6$. The cubic is represented by its coefficient vector $C \in \mathbb{R}^{20}$. Unlike in previous sections, this tropical cubic need not be tropically smooth. A pair (P, C) lies in $\text{Trop}(I_{\text{ufv}})$ if and only if $\text{in}_{(P,C)}(I_{\text{ufv}})$ contains no monomial. We take this initial ideal in the Laurent polynomial ring.

Example 6.1. The line given by $P = (26, 6, 17, 7, 18, 0)$ lies on the surface given by $C = (32, 17, 20, 41, 26, 17, 32, 33, 36, 54, 8, 1, 14, 4, 7, 18, 0, 0, 0, 0)$. This pair corresponds to the motif of type 3D in Example 3.3; see the diagram on the left-hand side of Figure 3. We verify the containment algebraically by checking that

$$(14) \quad \begin{aligned} \text{in}_{(P,C)}(I_{\text{ufv}}) = & \langle p_{03}p_{12} - p_{02}p_{13}, p_{01}c_5 - p_{12}c_8, p_{13}c_{14} + p_{12}c_{15}, \\ & p_{03}c_{14} + p_{02}c_{15}, p_{23}c_{15} + p_{13}c_{18}, p_{03}c_{11} + p_{13}c_{17}, \\ & p_{23}c_{14} - p_{12}c_{18}, p_{02}c_{11} + p_{12}c_{17} \rangle \end{aligned}$$

contains no monomial. This initial ideal lives in the Laurent polynomial ring. For instance, the ten terms in (13) have weights 68, 68, 73, 75, 75, 82, 85, 87, 95, 110 in this order, and the resulting initial form equals $(p_{01}c_5 - p_{12}c_8)p_{12}p_{13}$.

The point (P, C) lies in the relative interior of a maximal cell of $\text{Trop}(I_{\text{ufv}})$. The inequality description of this cell is read off from a Gröbner basis of I_{ufv} . For instance, the polynomial (13) contributes the equation $P_{01} + C_5 = P_{12} + C_8$ and eight inequalities, namely, $P_{01} + C_5 + P_{12} + P_{13}$ is bounded above by

$$\begin{aligned} & P_{01} + 2P_{12} + C_7, \quad 3P_{12} + C_9, \quad P_{12} + 2P_{13} + C_6, \quad P_{01} + 2P_{13} + C_2, \\ & 2P_{01} + P_{12} + C_4, \quad 2P_{01} + P_{13} + C_1, \quad 3P_{13} + C_3 \quad \text{and} \quad 3P_{01} + C_0. \end{aligned}$$

Such constraints, derived from polynomials in I_{ufv} , define the cells of $\text{Trop}(I_{\text{ufv}})$.

The maximal cones of $\text{Trop}(I_{\text{ufv}})$ represent occurrences of motifs in $3\Delta_3$. In particular, if we could compute this fan, then this would be an *ab initio* derivation of the motifs 3A, 3B, ..., 3J. These were found geometrically in [22].

Remark 6.2. Motifs and their occurrences can be identified from initial ideals $\text{in}_{(P,C)}(I_{\text{ufv}})$. For instance, the indices i of the unknowns c_i in (14) form the list $(A, B, C, D, E, F, G, H) = (11, 17, 18, 14, 15, 5, 8)$ we saw in Example 4.2.

Unfortunately, it is very difficult to compute with the ideal I_{ufv} . Even finding a single Gröbner basis is hard. For instance, the computation of (14) only terminated after we imposed some degree constraints in `Macaulay2`. One open problem naturally arising here is to find a tropical basis of I_{ufv} . The Schläfli fan fits into a broader theory, yet to be developed, for discriminants of morphisms in tropical algebraic geometry. We propose the following approach. Let \mathcal{X} be a tropical variety in $\mathbb{TP}^d \times \mathbb{TP}^n$ and ϕ the projection from \mathcal{X} onto the second factor \mathbb{TP}^n . We assume that ϕ is onto, so $\dim(\mathcal{X}) \geq n$. Let $\mathcal{X}^{(n-1)}$ be the subcomplex of \mathcal{X} consisting of all cells of dimension at most $n-1$. If this is the *ramification locus* then $\phi(\mathcal{X}^{(n-1)})$ plays the role of the *branch locus*.

Example 6.3. Tropical discriminants [5] are a special case of this construction. Let \mathcal{A} be a subset of $n+1$ elements in \mathbb{Z}^d . Consider hypersurfaces in d -space defined by Laurent

polynomials with these $n + 1$ terms. We write $C = (C_a : a \in \mathcal{A}) \in \mathbb{R}^{n+1}$ for the vector of coefficients, and $P = (P_1, \dots, P_d)$ for a point in \mathbb{R}^d . The *universal tropical hypersurface* is the tropical variety \mathcal{X} defined by

$$(15) \quad \bigoplus_{a \in \mathcal{A}} C_a \odot P^a = \bigoplus_{a \in \mathcal{A}} C_a \odot P_1^{\odot a_1} \odot P_2^{\odot a_2} \odot \dots \odot P_d^{\odot a_d}.$$

The map $\phi : \mathcal{X} \rightarrow \mathbb{R}^{n+1}/\mathbb{R}\mathbf{1}, (C, P) \mapsto C$ is surjective. The fiber $\phi^{-1}(C)$ is the hypersurface in \mathbb{R}^d whose tropical polynomial has coefficients C . The tropical variety \mathcal{X} has dimension $n + d - 1$. It is a fan with $\binom{n+1}{2}$ maximal cones, one for each pair of terms in (15). The subfan $\mathcal{X}^{(n-1)}$ consists of $\binom{n+1}{d+2}$ cones of dimension $n - 1$. On each cone, the minimum among the $n + 1$ terms in (15) is attained by a fixed set of $d + 2$ terms. Hence the regular subdivision of \mathcal{A} defined by C is not a triangulation. The image $\phi(\mathcal{X}^{(n-1)})$ consists of the cones of codimension ≥ 1 in the secondary fan of \mathcal{A} . In particular, the tropical discriminant defined above contains that of [5]. The difference arises from the distinction between the \mathcal{A} -discriminant and the principal \mathcal{A} -determinant; see [6] and [10].

Remark 6.4. The number of cones in $\mathcal{X}^{(n-1)}$ is much smaller than that of its image under the projection ϕ . This phenomenon is familiar from computer algebra (cf. elimination theory) and optimization (cf. extended formulations). In our context, take $\mathcal{A} = 3\Delta_3$ in Example 6.3. The universal cubic surface \mathcal{X} has only $\binom{20}{2} = 190$ maximal cones, whereas its discriminant $\phi(\mathcal{X}^{(n-1)})$ forms the walls between many more than 344 843 867 cones.

We now come to the main theoretical result in this section. The role of points will be played by lines. An analogous result holds for Fano varieties of arbitrary hypersurfaces (15). We focus on the case of cubic surfaces in \mathbb{TP}^3 .

Proposition 6.5. *Let $\mathcal{X} = \text{Trop}(I_{\text{ufv}})$ be the tropical universal Fano variety in $\mathbb{TP}^5 \times \mathbb{TP}^{19}$ and ϕ the map onto the second factor (space of tropical cubics). The tropical discriminant of ϕ is contained in the union of the codimension 1 cones in the Schläfli fan. The latter is a subset of the union of all Schläfli walls.*

Proof. All cubics C in the interior of one fixed Schläfli cone have the same visible motifs. The Plücker vectors P of the 27 lines are linear functions in the entries of C , as long as C stays within one Schläfli cone. Hence the set of cells in \mathcal{X} that are intersected by the fiber $\phi^{-1}(C)$ remains constant throughout that Schläfli cone. These cells all have the full dimension 19. In particular, $\phi^{-1}(C)$ is disjoint from $\mathcal{X}^{(18)}$ for C in the interior of a Schläfli cone. This shows that this interior is disjoint from the tropical discriminant of ϕ . \square

We conclude with a brief discussion of a related universal family. It lives in $\mathbb{P}^3 \times \mathbb{P}^{19}$, where \mathbb{P}^3 now parametrizes planes in the ambient 3-space. Each plane $\{u_0x_0 + u_1x_1 + u_2x_2 + u_3x_3 = 0\}$ intersects a cubic surface in a plane cubic curve. The plane is a *tritangent plane* if the plane cubic decomposes into three lines. The *universal Brill variety* is the 19-dimensional irreducible variety consisting of all pairs (u, f) , where $u = (u_0 : u_1 : u_2 : u_3)$ is a tritangent plane to the cubic surface $\{f = 0\}$. The map from this variety onto \mathbb{P}^{19} is a 45-to-1 covering, since a general cubic surface has 45 tritangent planes.

We introduce an ideal I_{bri} that defines the universal Brill variety. It lives in the ring $\mathbb{Q}[u_0, u_1, u_2, u_3, c_0, c_1, \dots, c_{19}]$, where the last ten unknowns are the coefficients of a ternary

cubic. In these unknowns, we consider the prime ideal of codimension 3 and degree 15 that defines the factorizable cubics. Its variety is an instance of a *Chow variety*, and the equations are known as *Brill equations* [10, §I.4.H]. This prime ideal is generated by 35 quartics in the 10 unknowns.

We now derive 35 generators of I_{bri} . Set $x_3 = -\frac{1}{u_3}(u_0x_0 + u_1x_1 + u_2x_2)$ in f , and clear denominators to get a ternary cubic with coefficients $\mathbb{Q}[u_0, u_1, u_2, u_3]$. We substitute these cubics into the Brill equations and we remove factors of u_3 . The resulting 35 polynomials of bidegree $(7, 4)$ in (u, c) generate our ideal I_{bri} .

We are interested in the resulting *tropical universal Brill variety*

$$\mathcal{X} = \text{Trop}(I_{\text{bri}}) \subset \mathbb{TP}^3 \times \mathbb{TP}^{19}.$$

Its points are pairs consisting of a tropical cubic and a tritangent plane. The maximal cones of $\text{Trop}(I_{\text{bri}})$ represent occurrences of *triple motifs* in $3\Delta_3$. It would be desirable to compute these. We note that the tritangent planes correspond to the 45 triangles in the *Schläfli graph*. This is the 10-regular graph whose vertices are the 27 lines, and whose edges are incident pairs of lines. The motifs and the triple motifs that occur in a triangulation can be seen as a tropical structure for annotating and extending the Schläfli graph.

Acknowledgements. We are very grateful to Lars Kastner, Benjamin Lorenz and Andreas Paffenholz for their help with the computations for this project. We thank Sara Lamboglia, Yue Ren and Emre Sertöz for their comments on a manuscript version of this article. We are also grateful to the two anonymous referees whose comments helped us improving the article. Michael Joswig was supported by Deutsche Forschungsgemeinschaft (EXC 2046: "MATH+", SFB-TRR 195: "Symbolic Tools in Mathematics and their Application", and GRK 2434: "Facets of Complexity").

REFERENCES

- [1] Altshuler, A., Steinberg, L.: Neighborly 4-polytopes with 9 vertices. *J. Combinatorial Theory Ser. A* **15**, 270–287 (1973)
- [2] Bogart, T., Katz, E.: Obstructions to lifting tropical curves in surfaces in 3-space. *SIAM J. Discrete Math.* **26**(3), 1050–1067 (2012)
- [3] Brugallé, E., Shaw, K.: Obstructions to approximating tropical curves in surfaces via intersection theory. *Canad. J. Math.* **67**(3), 527–572 (2015)
- [4] De Loera, J.A., Rambau, J., Santos, F.: *Triangulations, Algorithms and Computation in Mathematics*, vol. 25. Springer-Verlag, Berlin (2010)
- [5] Dickenstein, A., Feichtner, E.M., Sturmfels, B.: Tropical discriminants. *J. Amer. Math. Soc.* **20**(4), 1111–1133 (2007)
- [6] Dickenstein, A., Tabera, L.F.: Singular tropical hypersurfaces. *Discrete Comput. Geom.* **47**(2), 430–453 (2012)
- [7] <https://github.com/flyspeck/flyspeck>
- [8] Gawrilow, E., Joswig, M.: `polymake`: a framework for analyzing convex polytopes. In: *Polytopes – combinatorics and computation* (Oberwolfach, 1997), *DMV Sem.*, vol. 29, pp. 43–73. Birkhäuser (2000)
- [9] Geiger, A.: On realizability of lines on tropical cubic surfaces and the Brundu-Logar normal form. *Le Matematiche* (2020)
- [10] Gel'fand, I.M., Kapranov, M., Zelevinsky, A.: *Discriminants, Resultants, and Multidimensional Determinants*. Birkhäuser, Boston (1994)
- [11] Gleixner, A., et al.: The SCIP Optimization Suite 6.0. Technical report, Optimization Online (2018)

- [12] Grayson, D.R., Stillman, M.E.: `Macaulay2`, a software system for research in algebraic geometry. URL <http://www.math.uiuc.edu/Macaulay2/>
- [13] Hampe, S.: `a-tint`: a `polymake` extension for algorithmic tropical intersection theory. *European J. Combin.* **36**, 579–607 (2014)
- [14] Hampe, S., Joswig, M.: Tropical computations in `polymake`. In: *Algorithmic and experimental methods in algebra, geometry, and number theory*, pp. 361–385. Springer, Cham (2017)
- [15] Hampe, S., Joswig, M., Schröter, B.: Algorithms for tight spans and tropical linear spaces. *J. Symbolic Comput.* **91**, 116–128 (2019)
- [16] Jordan, C., Joswig, M., Kastner, L.: Parallel enumeration of triangulations. *Electron. J. Combin.* **25**(3), Paper 3.6, 27 (2018)
- [17] Joswig, M., Panizzut, M., Sturmfels, B.: `polymake` extension `TropicalCubics`. <https://polymake.org/extensions/tropicalcubics>
- [18] Maclagan, D., Sturmfels, B.: Introduction to tropical geometry, *Graduate Studies in Mathematics*, vol. 161. American Mathematical Society, Providence, RI (2015)
- [19] McKay, B., Piperno, A.: Practical graph isomorphism, II. *J. Symbolic Comput.* **60**, 94–112 (2014)
- [20] Paffenholz, A.: `polyDB`: a database for polytopes and related objects. In: *Algorithmic and experimental methods in algebra, geometry, and number theory*, pp. 533–547. Springer, Cham (2017)
- [21] Panizzut, M., Sertöz, E., Sturmfels, B.: An octanomial model for cubic surfaces. *Le Matematiche* (2020)
- [22] Panizzut, M., Vigeland, M.: Tropical lines on smooth tropical surfaces (2019). [arXiv:0708.3847](https://arxiv.org/abs/0708.3847)
- [23] Schläfli, L.: An attempt to determine the twenty-seven lines upon a surface of the third order, and to divide such surfaces into species in reference to the reality of the lines upon the surface. *Quarterly Journal of Pure and Applied Mathematics* **2**, 55–65 (1858)
- [24] Vigeland, M.: Smooth tropical surfaces with infinitely many tropical lines. *Ark. Mat.* **48**(1), 177–206 (2010)

(M. Joswig) TU BERLIN, GERMANY

E-mail address: joswig@math.tu-berlin.de

(M. Panizzut) TU BERLIN, GERMANY

E-mail address: panizzut@math.tu-berlin.de

(B. Sturmfels) MPI LEIPZIG, GERMANY AND UC BERKELEY, USA

E-mail address: bernd@mis.mpg.de